

## Numerical Brownian-motion model reaction rates\*

P. B. Visscher<sup>†</sup>

*Department of Physics, University of California at San Diego, La Jolla, California 92093*

(Received 9 February 1976)

This paper presents detailed numerical calculations of surface-catalyzed chemical reaction rates in the Brownian-motion rate theory of Kramers. Accurate values of the rate for a wide range of values of the friction coefficient, the principal parameter of the theory, are obtained for the first time. A one-parameter empirical formula is obtained which gives the rate in quite general circumstances. Application of the results to calculation of catalytic rates at metal surfaces is discussed.

### I. INTRODUCTION

In this paper we explore the consequences of the Brownian-motion approach to rate theory, proposed by Kramers.<sup>1</sup> Considerable effort has been expended towards justifying the application of the Brownian-motion model to catalytic rates at metal surfaces<sup>2-5</sup> and towards calculating the friction coefficient needed to apply the model to such a surface.<sup>6,7</sup> It is, therefore, desirable to know the reaction rate predicted by this model, as a function of friction coefficient.

Good approximate solutions have been obtained for the limits of very large<sup>1</sup> and very small<sup>1,8,9</sup> friction; in both limits the rate was found to become small. So the case of greatest practical interest (i.e., highest reaction rate) is that of intermediate friction, for which the reaction rate goes through a maximum. No accurate calculation has previously been done in this region, and it is the purpose of this paper to present accurate numerical results for this case. Together with the previous results for the small- and large-friction limits, this provides an essentially complete picture of the dependence of reaction rates on friction.

### II. BROWNIAN THEORY OF CATALYTIC RATES

In the Brownian-motion theory<sup>1,10</sup> of surface catalysis, the problem of determining the rate of a catalytic reaction is approximately reduced to that of determining the rate of escape of a Brownian particle from a one-dimensional potential well.<sup>3</sup> Consider a system consisting of a reacting complex (i.e., one molecule in the case of a unimolecular reaction, two in a biomolecular one, etc.) held on a solid surface by an attractive potential. Temporarily ignoring the internal degrees of freedom of the surface (phonons and electronic excitations), we can calculate the Born-Oppenheimer energy surface for the complex in the potential field of the static solid (i.e., the energy of

the system as a function of the nuclear coordinates of the atoms in the complex). In general, the reactant and product of the catalyzed reaction correspond to two minima of this Born-Oppenheimer energy function. If the reacting complex is weakly coupled to the individual internal degrees of freedom of the solid surface (though it may be held tightly by the time-independent attractive potential of the surface), the influence of the internal degrees of freedom on the atoms of the complex may be approximated by a frictional force and a Markoffian random force acting on each of the atoms, just as in classical Brownian motion.<sup>11</sup> Furthermore, our interest is in systems moving in many-body configuration space from the reactant minimum of the energy function to the product minimum, near a line (the reaction path) connecting these minima. We may transform to a curvilinear coordinate system<sup>12,13</sup> in which one coordinate (the reaction coordinate) increases along the path, and the other axes are orthogonal to it. If the friction along the orthogonal coordinates is sufficient to maintain thermal equilibrium along these directions, they may be factored out of the problem, leaving us with a one-dimensional problem of escape from a potential well  $V(x)$  by a "particle" (representing the reacting system) whose position  $x$  and velocity  $v$  obey a Langevin equation

$$\frac{dv}{dt} = F(x) - \eta v + A(t), \quad (2.1)$$

where  $F(x) = -(1/m)(\partial V/\partial x)$ ,  $m$  is the effective mass,  $\eta$  is the effective friction coefficient, and  $A(t)$  is a Markoffian random force with zero correlation time [reasonable if the internal degrees of freedom of the substrate giving rise to  $\eta$  and  $A(t)$  vary rapidly compared to  $x$  and  $v$ ]. An ensemble of such systems then obeys a Fokker-Planck equation<sup>11</sup>

$$\frac{\partial f}{\partial t} + v \frac{\partial f}{\partial x} + F \frac{\partial f}{\partial v} = \eta \frac{\partial}{\partial v} \left( v f + \frac{kT}{m} \frac{\partial f}{\partial v} \right), \quad (2.2)$$

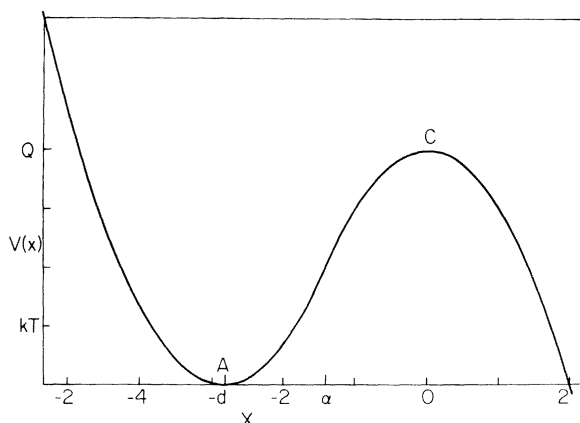


FIG. 1. Potential well [Eq. (2.3)] used for numerical calculations of escape rate. Distance is measured in the dimensionless units described in the text; for this case  $\alpha = -2^{1/2}$ ,  $d = +2^{3/2}$ .

where  $f(x, v, t)$  is the ensemble distribution function.

The choice of a potential  $V(x)$  requires some care. The potential along the reaction path in many-particle configuration space goes from one minimum to another. It would seem appropriate to use a one-dimensional  $V(x)$  with two minima, a "double well." However, it is clear that in a real reaction only the reactant well and the barrier region are important; what happens after the "particle" has entered the product well is irrelevant. This is true numerically in the case of large friction, when the distribution diffuses very slowly into the product well. The reaction-rate constant can be computed as the ratio of the leakage rate to the reactant well population. After some density has built up in the product well, backflow into the reactant well can occur, but this is a real physical effect (the reverse reaction), and the populations of the two wells obey simple first-order kinetic equations, involving the rate constant mentioned above. In the small-friction case, however, the true rate is harder to define. A particle in the reactant well with enough energy to surmount the barrier will do so, entering the product well. But it is then quite likely to bounce right back into the reactant well, since the frictional energy loss is small. This is *not* a physical effect, but an artifact of the assumed one dimensionality. In the real many-dimensional configuration space, a particle escaping into the product well along the reaction path is going in a specific direction, and the chance that the forces in the product well will send it back along exactly the same path is very small. The "backflow" effect in the model is spurious; if it is to describe a real reaction between well-defined chemical species, the particle must be

trapped in the product well, and the details of the trapping must be irrelevant.

Thus, for both large and small friction, the nature of the product well is irrelevant, and for the small friction case it must not be allowed to reflect particles. This is achieved by the well shown in Fig. 1; the barrier potential continues downward indefinitely on the product side.

The potential used in the numerical calculations consists of an upward parabolic well and a downward parabolic barrier:

$$V(x) = \begin{cases} \frac{1}{2} m \omega_A^2 (x+d)^2 & (x < \alpha) \\ Q - \frac{1}{2} m \omega_C^2 x^2 & (x > \alpha) \end{cases} \quad (2.3)$$

The separation  $d$  and the inflection point  $\alpha$  are uniquely determined by  $Q$ ,  $\omega_A$ ,  $\omega_C$ . Thus these three variables, with  $kT$ ,  $m$ , and  $\eta$ , determine the problem uniquely.

If we pick units  $\omega_A$  for time,  $kT$  for energy ( $2kT/m$ )<sup>1/2</sup> for velocity, the only remaining variables are  $Q/kT$ ,  $\omega_C/\omega_A$ , and  $\eta/\omega_A$ . For the numerical calculations we chose  $\omega_C = \omega_A$  and  $Q/kT = 4$ , and allowed  $\eta$  to vary. We indicate in Sec. VD how the results might be extrapolated to larger  $Q/kT$ ; this has not yet been checked by doing numerical calculations at larger  $Q/kT$ , but that would not be difficult.

To calculate a reaction-rate constant, we consider an ensemble  $f(x, v, t)$  in which particles are being injected into the reactant well at the rate  $\lambda(x, v)$ . [Such injection modifies the Fokker-Planck Eq. (2.2) by introducing a term  $\lambda(x, v)$  on the right.] When the system reaches a steady state  $f_s(x, v)$ , the rate constant is the ratio of the current of particles over the barrier to the population of the well

$$r = j_s / N_s, \quad (2.4)$$

where

$$j_s = \int_{-\infty}^{\infty} f_s(0, v) v dv, \quad (2.5)$$

$$N_s = \int_{-\infty}^0 dx \int_{-\infty}^{\infty} dv f_s(x, v). \quad (2.6)$$

Physically, the injection distribution  $\lambda(x, v)$  is determined by the phase-space distribution of molecules which adsorb on the surface. For the purposes of this calculation, we will assume it is a Boltzmann distribution for  $x < 0$ , and zero for  $x > 0$ :

$$\lambda(x, v) = \begin{cases} \exp\{-[\frac{1}{2}mv^2 + V(x)]/kT\} & (x < 0) \\ 0 & (x > 0) \end{cases} \quad (2.7)$$

The sharp cutoff of  $\lambda$  at  $x=0$  is somewhat arbitrary, as is the cutoff of the integral in Eq. (2.6). However, the fraction of the density in  $\lambda$  or  $f$  near

$x=0$  is of order  $e^{-Q/kT}$ , which is negligibly small in practice, so the cutoffs have little effect and may be chosen where it's most convenient.

In fact, instead of calculating a steady state  $f_s(x, v)$ , the calculation was done with a transient state having initial condition

$$f(x, v, t=0) = \lambda(x, v) / \omega_A. \quad (2.8)$$

This amounts to replacing the steady source  $\lambda(x, v)$  by the impulsive source  $\lambda(x, v)\delta(t)/\omega_A$ , which inserts particles only at  $t=0$  (the factor  $\omega_A$  is included so the units of the sources agree). This was done partly for numerical convenience [we can merely step  $f(x, v, t)$  forward in time, and needn't solve an implicit equation for  $f_s(x, v)$ ], and partly because there is some interest in the transient behavior (see Sec. V B). Clearly the steady source is recovered by integrating the new source over time, so the steady-state solution  $f_s$  is the corresponding superposition of transient solutions:

$$f_s(x, v) = \omega_A \int_0^\infty f(x, v, t) dt, \quad (2.9)$$

so we can retrieve the steady-state rate constant as

$$r = \int_0^\infty dt j(t) / \int_0^\infty dt N(t) \quad (2.10)$$

from the transient current and population  $j(t)$ ,  $N(t)$ , defined analogously to Eqs. (2.5) and (2.6).

### III. NUMERICAL TECHNIQUES

To calculate the reaction rate [Eq. (2.10)] we must know the time evolution of the distribution function  $f(x, v, t)$ , which is determined by the Fokker-Planck equation (2.2). The algorithm used for the solution of this first-order linear partial differential equation is described in detail elsewhere.<sup>14</sup> It involves expanding the velocity dependence of  $f(x, v, t)$  in Hermite polynomials  $H_n$ :

$$f(x, v, t) = \sum_{n=0}^{n_{\max}} a_n(x, t) H_n(v) e^{-v^2}. \quad (3.1)$$

[As in Sec. II,  $v$  is in units of  $(2kT/m)^{1/2}$ .]

This is physically very reasonable for large  $\eta$ , when the velocity distribution is nearly Maxwellian [i.e., the first term dominates Eq. (3.1)]. We can then cut off the summation at a low order  $n_{\max}$ . In fact, truncating the calculation at  $n_{\max} = 1$  [two terms of Eq. (3.1)] corresponds exactly to the Smoluchowski equation,<sup>3,11</sup> which is correct in the large- $\eta$  limit. For low  $\eta$ , this expansion becomes increasingly awkward, and in fact for  $\eta = 0.1$   $\omega_A$  convergence was not achieved even with  $n_{\max} = 40$ .

The Hermite-function expansion converts the partial differential equation in three variables into

a set of coupled equations in two variables.<sup>3</sup> These are then solved on a grid of points in  $x$  and  $t$ , after replacing derivatives by finite differences. To avoid numerical instabilities described in Ref. 14, it is necessary to define the odd and even coefficients  $a_n$  on different grids in  $x$ , and to use a Runge-Kutta method for stepping in  $t$ .

Because of our choice [Eq. (2.7)] of a discontinuous initial condition, highly singular distributions in both  $x$  and  $v$  are present near  $t=0$ . These create numerical oscillations for early times. The spurious oscillations are largely independent of the potential, however, and by calculating them exactly for the force-free case<sup>15</sup> it has proved possible to subtract them out.

Reflecting boundary conditions are most natural for this algorithm. This creates no problems on the left side of Fig. 1, where the boundary can be chosen to have  $V(x)$  so large there are virtually no particles to reflect. At the right, however, reflection is a serious problem which was solved by

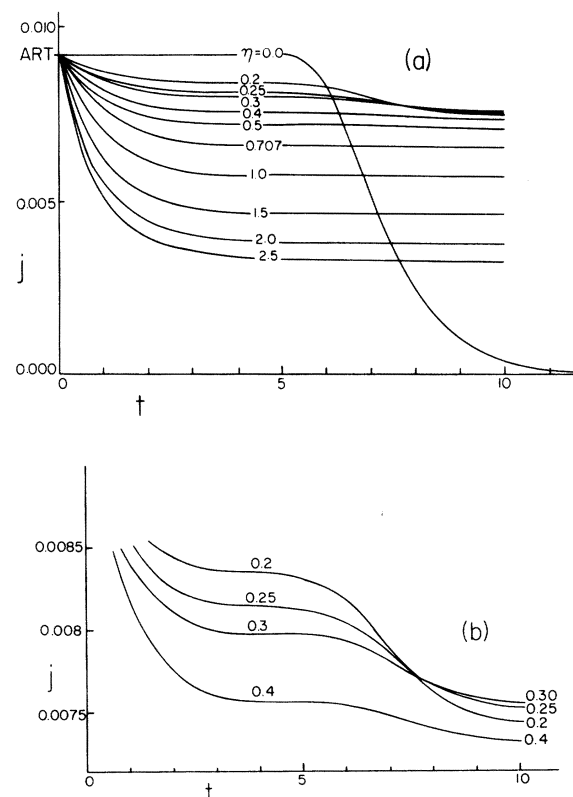


FIG. 2. (a) Numerical results for current across barrier, labeled by friction coefficient  $\eta$  (in units of the well frequency  $\omega_A$ ). ART labels the absolute-rate-theory value  $\frac{1}{2} e^{-Q/kT}$ . The  $\eta=0$  result was obtained analytically:  $j(t) = \frac{1}{2} (e^{-Q/kT} - e^{-E(t)/kT})$ , where  $E(t)$  is the energy of a trajectory traversing the  $x < 0$  region in time  $t$ . (b) Expanded vertical scale ( $5\times$ ) showing drop of low- $\eta$  curves around  $t = 6$ .

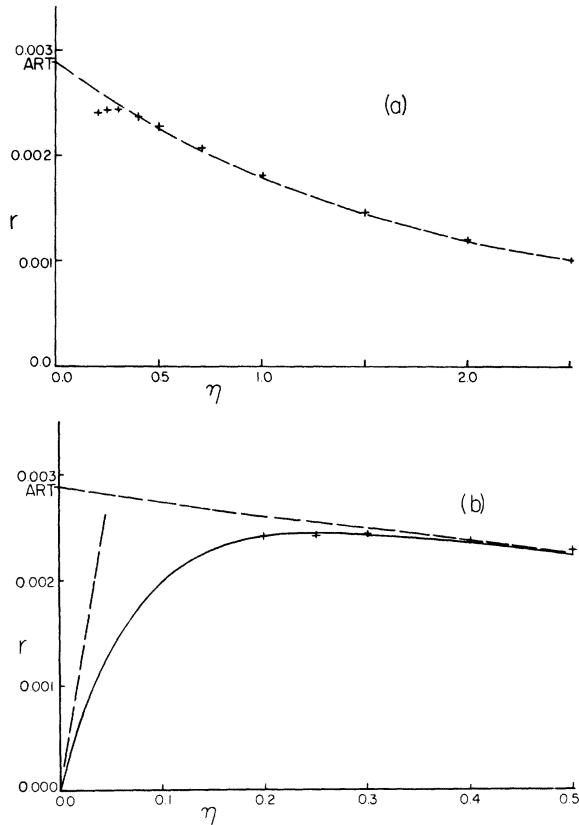


FIG. 3. (a) Rate constant  $r$  [Eqs. (2.4) or (2.10)] as a function of friction coefficient  $\eta$  (in units of  $\omega_A$ ). Crosses are numerical results, dashed line is Kramers's large- $\eta$  solution, Eq. (5.1). ART rate [Eq. (5.2)] is indicated. (b) Expanded horizontal scale (5 $\times$ ) showing small- $\eta$  approximation (Ref. 8) as dashed line through origin, and parametric fit [Eq. (5.5)] as solid curve.

attaching a steep parabolic well to  $V(x)$  at a point  $x_R > 0$ , and increasing the friction to a large value in the bottom of this extra well to form a trap. Very few particles then reach the reflecting barrier, on the right side of this extra well. By increasing  $x_R$  and the depth of the trap until the resulting current no longer changed, the result for the unbounded potential (2.3) was obtained.

#### IV. NUMERICAL RESULTS

For various values of the friction coefficient  $\eta$ , the discrete algorithm described above was used to calculate the evolution of  $f(x, v, t)$  for  $0 < t < t_{\max}$ , with initial condition given by Eqs. (2.8) and (2.7). This then yielded the population  $N(t)$  of the well and the escaping current  $j(t) = -(d/dt)N(t)$ , shown in Fig. 2. (The dimensionless units used are defined in Sec. II.) All the  $j(t)$  curves start at the same value,  $\frac{1}{2}e^{-Q/kT}$ . This is the value predicted by the equilibrium, or "absolute rate," theory<sup>1</sup>; it corresponds to a thermal-equilibrium distribu-

tion of particles flowing to the right, and none at all flowing to the left. The current starts at this value because of our singular initial condition: equilibrium for  $x < 0$ , zero density for  $x > 0$ . The current then slows down at a rate proportional to the friction coefficient.

We now describe how the rate constant, shown in Fig. 3, was obtained from the current data in Fig. 2. In general, the evolution of  $f(x, v, t)$  can be expressed in terms of the eigenfunctions of the Fokker-Planck equation (2.2). This leads to an expression for the current of the form

$$j(t) = A_1 e^{-\lambda_1 t} + A_2 e^{-\lambda_2 t} + \dots, \quad (4.1)$$

where  $\lambda_1, \lambda_2, \dots$ , are the eigenvalues. Evidently, the first term is the most important; it dominates after a long time, and describes the slow leakage of particles from the well. The rest of Eq. (4.1) will be referred to as the "transient" and may not be conveniently described by the series (4.1) for small  $t$  (i.e., the series may not converge well; also some eigenvalues may be complex.) In any event there is a characteristic time for the dying out of the transient, which has been referred to as the "attainment time,"<sup>16</sup> and is equal to  $\lambda_2^{-1}$  if the transient is described by a rapidly converging Eq. (4.1). This is the time required for the distribution to attain the asymptotic decay rate  $\lambda_1$ . Note that as  $t \rightarrow \infty$ ,  $\lambda_1 = \lim_{t \rightarrow \infty} j(t)/N(t)$ , which is almost the rate constant  $r$  [Eq. (2.10)], except for a correction due to the transient, which is small in the usual case of small  $r$ .

The time  $t_{\max}$  was chosen large enough so that the tails of all the curves  $j(t)$  could be fit to the first two terms of Eq. (4.1) to within the numerical error of about  $\frac{1}{2}\%$ ;  $t_{\max} = 10$  was sufficient. This fit was used to extrapolate  $j(t)$  beyond  $t_{\max}$ , which is necessary in order to use Eq. (2.10) to extract the rate constant from the data in Fig. 2. The second term is very small for  $t > t_{\max}$ , so Fig. 2 effectively shows the entire transient region. Beyond  $t = t_{\max}$ , the current just decays exponentially as  $\exp(-\lambda_1 t)$ . It appears to reach a limit because  $\lambda_1^{-1} \gg t_{\max}$ ; the decay is barely beginning by  $t = t_{\max}$ .

In fitting  $j(t)$  to Eq. (4.1), the four variables  $\lambda_1$ ,  $A_1$ ,  $\lambda_2$ , and  $A_2$  may not be varied independently, because of the constraint

$$N(0) - \int_0^\infty j(t) dt = N(\infty) = 0, \quad (4.2)$$

where

$$N(0) \approx 3.178 \quad (4.3)$$

is the initial population of the well ( $\pi$  for a pure parabolic well). Fitting  $j(t)$  subject to this constraint determines  $\lambda_1$  and  $A_1$  very accurately;  $\lambda_1$

is mostly determined by (4.2), and  $A_1$ ,  $\lambda_2$ , and  $A_2$  mostly by the fit. For example, with  $\eta=2$  (in units in which  $\omega_A=1$ ) we have for  $t>2$

$$j(t) \approx 0.00378e^{-0.00119t} + 0.00441e^{-0.99t}, \quad (4.4)$$

and with  $\eta=0.2$ , we have for  $t>8$

$$j(t) \approx 0.00761e^{-0.00240t} + 0.287e^{-1.00t}. \quad (4.5)$$

The extrapolation (4.1) for  $j(t)$  then allows us to compute the rate constant  $r$  analytically from (2.10); the results are plotted as Fig. 3. The rate constant turns out to depend mostly on  $j(t_m)$ ; in fact  $\lambda_1 N(0)$ ,  $A_1$ , and  $rN(0)$  are all (within a few percent) equal to  $j(t_m)$ . So one can conveniently interpret the values  $j(t_m)$  at the right edge of Fig. 2 as being proportional to the rate constants for the various friction coefficients.

## V. DISCUSSION

### A. Relation to Kramers' theory

The rate constant for the Brownian-motion theory was calculated exactly for the pure parabolic barrier by Kramers<sup>1</sup>:

$$r_K = \frac{1}{2}e^{-Q/kT}[(1 + \eta^2/4\omega_C^2)^{1/2} - \eta/2\omega_C]/N(0) \quad (5.1)$$

[in units of  $\omega_A$ , as above;  $N(0)$  is the equilibrium population of the well, given in our case by Eq. (4.3)]. This was expected to correctly describe escape from a well for large friction coefficient  $\eta$ , because the velocity equilibration rate is then rapid and the depletion of the equilibrium distribution on the left slope of the barrier by the barrier leakage is easily compensated by diffusion from the well to its left, the fact that the well has finite depth has little effect.

This clearly cannot remain true for low  $\eta$ ; for  $\eta=0$  the particles with  $E>Q$  will escape, leaving the bulk of the particles having  $E<Q$  trapped in the well, unable to escape in any finite time. The equilibrium rate constant is thus zero. For low  $\eta$ , the escape rate depends on particles accelerated from  $E<Q$  to  $E>Q$  by the stochastic force, a sort of diffusion in energy. Kramers made an estimate for the rate based on this picture, in which the rate is proportional to  $\eta$ . Improvements have been made on this calculation,<sup>8,9</sup> leading to a somewhat larger proportionality constant.

Based on these two limits, shown as dashed curves in Fig. 3, Kramers conjectured that there would be a wide range of  $\eta$  in which the rate is given quite well (within 10%) by the absolute-rate-theory (ART) value<sup>1</sup>

$$r_{\text{ART}} = \frac{1}{2}e^{-Q/kT}N(0). \quad (5.2)$$

This conclusion depends crucially on how the rate interpolates between the two limits; Kramers

assumed the actual rate follows each curve until quite near their intersection.

The objective of the present calculation was to calculate the rate in the interpolation region, in particular, to try to locate the maximum. As Fig. 3 shows, this was achieved, and the result lends some support to Kramers's conjecture: the rate peaks quite near the ART value (though not within 10%). An extrapolation of the results to larger, more realistic barrier heights (described below) can put the result very near the ART value.

### B. High friction

The agreement between the numerically computed rates and Kramers's high- $\eta$  limit is extremely close. [Kramers's rate is even closer to the calculated long-time limit of  $j(t)/N(t)$ ; the rate  $r$  exceeds this slightly due to the transient.] This provides encouraging evidence for the correctness of the solution algorithm. The agreement persists down to  $\eta$ 's which are by no means large compared, say, to  $\omega_A (=1)$ ; Kramers's approximation was indeed well chosen.

It can be seen from Fig. 2 that the attainment times are roughly the same for all the large-friction cases ( $\eta \geq 1$ ). In fact, the fitted values of  $\lambda_2^{-1}$  are all equal to 1, within the ambiguity ( $\pm 10\%$ ) introduced because they depend on the exact interval used for fitting. (This is even true for the low-friction cases, where, however,  $\lambda_2^{-1}$  describes only the exponential decay at the far right; the total attainment time is discussed below.)

The friction independence of the attainment time is of interest because of a previous suggestion,<sup>16</sup> based on an approximate theory of the attainment time, that it becomes anomalously large at  $\eta = 2^{-1/2}$ . It is apparent from Fig. 2 that this does not occur. However, a new phenomenon does become apparent at about this value of  $\eta$ , which has the effect of increasing the attainment time; this is discussed in Sec. VC.

### C. Low friction

For  $\eta \leq 0.707$ , the current  $j(t)$  appears to level off by around  $t=3$ , but then abruptly drops to a lower value around  $t=6$ . The plateau to  $t \approx 3$  corresponds to Kramers's exact solution for the pure parabolic barrier (dashed curve in Fig. 3); it has clearly not yet felt the effect of the finiteness of the well to the left.

For large friction,  $j(t)$  never does feel this effect. The way in which it is felt for small friction can be seen for  $\eta=0$  which is exactly solvable. The current in this case is due to particles on trajectories with energy  $E>Q$ , which started out at  $x<0$ . The particles on a particular trajectory

will sweep around that trajectory in the well, contributing a constant current across the barrier until the last particle (one which was just entering the well at  $t=0$ ) crosses and the current drops suddenly to zero. The time required for traversing the well depends on the trajectory, which smooths the current drop as in Fig. 2, but the average time is comparable to a period of oscillation in the harmonic well (namely  $2\pi$ ). It seems clear that the current drops around  $t=6$  for  $0 < \eta \leq 0.707$  are due to the same mechanism as for  $\eta=0$ , but less precipitous because the stochastic force continually promotes particles from trapped trajectories ( $E < Q$ ) to escape trajectories ( $E > Q$ ) to replace those lost.

#### D. Extrapolation to higher barriers

We give here a physically motivated parameterization with only one parameter of the rate  $r(\eta)$  which reproduces the numerical data and agrees well with the approximate solution in the low- $\eta$  limit (dashed line in Fig. 3). This enables extrapolation of our results to different potentials, in particular those with higher barriers. The parametric form of  $r(\eta)$  is based on Kramers's large- $\eta$  expression [Eq. (5.1)]. This is essentially exact for large  $\eta$ ; we wish to examine how it fails for smaller  $\eta$ .

We consider the current  $j(t)$  at a time after the transient has decayed; recall that this is essentially proportional to the rate constant. Consider a particle contributing to  $j(t)$ , i.e., leaving the well at time  $t$ , with velocity  $v$ . It lies on a trajectory passing in and out of the well, traversing the well in some time period  $\tau$ ; a particle on that trajectory would have entered the well at  $t-\tau$ , with velocity  $-v$ . (We have chosen  $t$  large enough so  $t > \tau$ .) In the absence of friction, this determines the distribution function at  $t$ : by Liouville's theorem,

$$f(0, v, t) = f(0, -v, t - \tau), \quad (5.3)$$

which is zero because particles only leave the well, never enter it. For nonzero friction  $\eta$  this is no longer exact; the stochastic force scatters particles away from their original trajectories. However, if  $\eta$  is small  $f(0, v, t)$  still retains some "memory" of  $f(0, -v, t - \tau)$  (which is nearly zero for small  $\eta$ ).

We assume this memory decays with time in an exponential fashion: in time  $\tau$ , it has decayed by  $e^{-A\eta\tau}$  for some constant  $A$  (since the decay rate clearly should be proportional to  $\eta$ ). Thus the distribution at  $t$ , which is the Kramers solution  $f_K(x, v)$  in the absence of memory and which decreases proportionately to the amount of memory ( $e^{-A\eta\tau}$ ) to zero for complete memory, is in general

$$f = f_K - e^{-A\eta\tau} f_K. \quad (5.4)$$

The corresponding current gives us the rate constant

$$r = r_K - e^{-A\eta\tau} r_K. \quad (5.5)$$

This has the correct behavior: it approaches the Kramers rate for large  $\eta$  and is linear in  $\eta$  for small  $\eta$ ,

$$r \rightarrow A\eta\tau r_{\text{ART}}. \quad (5.6)$$

This suggests what the dependence of  $A\tau$  on the barrier height should be, since Kramers's low- $\eta$  solution gives

$$r \propto \eta(Q/kT) r_{\text{ART}}. \quad (5.7)$$

So  $A\tau = B(Q/kT)$  for some constant  $B$ . The final parameterization is

$$r = (1 - e^{-B(Q/kT)\eta}) r_K, \quad (5.8)$$

where  $r_K$  is given by Eq. (5.1). The arbitrary parameter  $B$  may be fixed by requiring Eq. (5.8) to be correct at  $\eta=0.2$ ; this gives  $B=3.04$ . Then (5.8) is correct within 1% at *all* values of  $\eta$ ; it is plotted as the solid line in Fig. 3(b). As an independent check we can calculate the slope of (5.8) at  $\eta=0$ ; it is 0.035, compared to 0.073 in Kramers' approximate solution<sup>1</sup> and 0.057 in the improved solution.<sup>8</sup> This is adequate agreement, considering the uncertainties in the low- $\eta$  solution.

## VI. CONCLUSION

Numerical results have been given which fill the gap in previous calculations of reaction rates in the Brownian-motion model. A semiempirical formula [Eq. (5.8)] was found which reproduces the numerical results (and Kramers's high-friction limit<sup>1</sup>) very accurately, and gives good agreement with approximate low-friction calculations.

It would appear that the dependence of reaction-rate constants on friction coefficients is now adequately well known, and the next step in applying the Brownian-motion model to surface catalytic reactions must be the determination of  $\eta$  in a realistic situation. Previous attempts to do this in very simplified models<sup>6,7</sup> have given results highly dependent on details of the model. This suggests that perhaps an *a priori* calculation is too difficult, and one should instead determine  $\eta$  from an observed rate. One could then hope to predict other rates on the same substrate (assuming the same  $\eta$ ) with different barrier heights.

## ACKNOWLEDGMENT

The author would like to thank Professor H. Suhl for his help and advice during this work.

\*Work supported by a grant from NSF DMR74-03838.

† Present address: Institute for Theoretical Science, University of Oregon, Eugene, Or. 97403.

<sup>1</sup>H. A. Kramers, *Physica* 7, 284 (1940).

<sup>2</sup>Pradeep Kumar and Harry Suhl, *Phys. Rev. B* 5, 4664 (1972).

<sup>3</sup>E. G. d'Aglialo, W. L. Schaich, P. Kumar, and H. Suhl, in *Nobel Symposium 24, Collective Properties of Physical Systems*, edited by B. Lundquist (Academic, New York, 1973), p. 200.

<sup>4</sup>W. L. Schaich, *J. Chem. Phys.* 60, 1087 (1974).

<sup>5</sup>E. G. d'Aglialo, P. Kumar, W. Schaich, and H. Suhl, *Phys. Rev. B* 11, 2122 (1975).

<sup>6</sup>K.-P. Bohnen, M. Kiwi, and H. Suhl, *Phys. Rev. Lett.* 34, 1512 (1975).

<sup>7</sup>W. L. Schaich, *Phys. Lett. A* 50, 155 (1974); *Surf. Sci.* 49, 221 (1975).

<sup>8</sup>P. B. Visscher, *Phys. Rev. B* 13, 3272 (1976).

<sup>9</sup>W. Brenig, H. Müller, and R. Sedlmeier, *Phys. Lett.*

*A* 54, 109 (1975).

<sup>10</sup>In addition to surface catalysis, Brownian-motion rate theories have been applied to other problems such as diffusion in solids [G. H. Vineyard, *J. Phys. Chem. Solids* 3, 121 (1957); J. H. Weiner and R. E. Forman, *Phys. Rev. B* 10, 315 (1974)], and to the uncoiling of DNA [P. G. de Gennes, *J. Stat. Phys.* 12, 463 (1975)].

<sup>11</sup>S. Chandrasekhar, *Rev. Mod. Phys.* 15, 1 (1943).

<sup>12</sup>H. Suhl, *AIP Conf. Proc.* 18, 33 (1973).

<sup>13</sup>R. A. Marcus, *J. Chem. Phys.* 45, 4500 (1966).

<sup>14</sup>P. B. Visscher (unpublished).

<sup>15</sup>If  $V(x) \equiv 0$ , then  $f(x, v, t) = \exp(-v^2/v_0^2) \operatorname{erfc}[(\eta x - v - v_0 e^{-\eta t})/v_0]$  exactly, where  $\operatorname{erfc}$  is the complementary error function,  $v_0 = (2kT/m)^{1/2}$ ,  $v_1 = v_0(4e^{-\eta t} - e^{-2\eta t} + 2\eta t - 3)^{1/2}$ . Subtracting this from the numerical solution for  $V(x) \equiv 0$  gives the desired correction.

<sup>16</sup>H. Suhl and P. B. Visscher, *Jpn. J. Appl. Phys. Suppl.* 2, Pt. 2, 131 (1974).